Orbit Determination of Mars-Crossing Asteroid 699 Hela

Morgyn Judkins-Cooper,* Nicla Marabito,* and Samuel Yuan*
Summer Science Program (SSP) and Sommers-Bausch Observatory, University of Colorado Boulder, Boulder, CO 80309, USA
(Team 8: Briezy)
(Dated: 16 July 2024)

Maintaining an accurate catalog of planet-crossing asteroid orbits is critical to correct asteroid hazard assessment. We contribute to this effort with this work by observationally determining the orbit of Mars-crossing asteroid 699 Hela with Gauss' method. To do so, we observed 699 Hela over the course of 2.5 weeks and determined three best observations from which we computed its orbital elements. The determined orbital elements of asteroid 699 Hela at Julian Date 2460500.68896 were $a = 2.61 \pm 0.12$AU, $e = 0.410 \pm 0.027$, $i = 15.29 \pm 0.19^\circ$, $\Omega = 242.50 \pm 0.12^\circ$, $\omega = 91.4 \pm 2.2^\circ$, and $M = 321.1 \pm 4.1^\circ$. Empirically, we obtain low $\sim 1.079\%$ error in right ascension and $\sim 0.001\%$ error in declination on ephemeris generation consistency checks. The results of this work serve to refine the known orbit of asteroid 699 Hela.

Keywords: asteroids, Mars-crossing asteroids, celestial mechanics, orbit determination

I. INTRODUCTION

There are many forms of space debris in the solar system. Some of the most noticeable debris are asteroids and comets. Comets originate from the Oort Cloud, a shell of icy comet-like objects surrounding the solar system beyond Pluto and at the end of the Kuiper belt [1]. It is a common occurrence that these objects leave the cloud and enter the inner solar system. As the comet approaches the sun the ice melts and trails behind the comet becoming its tail [2]. Most asteroids are clustered in a region between Mars and Jupiter—the "main belt"—and generally pose no risk to Earth. Asteroids in the inner solar system, though, are of greater concern: due to their closer proximity to Earth and greater impact likelihood, tracking and refining their orbits is important for performing accurate hazard assessment [3].

Identifying and tracking the orbits of these inner solar system asteroids is difficult: many asteroids on collision courses with the earth are only detected hours before collision, as for asteroids 2008 TC3, 2014 AA, 2018 LA, and 2019 MO [4]. Furthermore, only 0.1% of Chelyabinsk-sized asteroids and 1% of Tunguska-sized "extinction" asteroids are tracked. Campaigns such as the B612 Foundation's Asteroid Institute aim to track these inner solar system asteroids and also educate the general public about the importance of these efforts [5].

Refining the orbits of these inner solar system asteroids is also critical to accurate tracking. In the case of asteroid 99942 Apophis—which was originally thought to be an asteroid with an extremely high impact likelihood—repeated observation and known-orbit refinement efforts have allowed accurate hazard assessment to be performed and fears of collision to be assuaged [6].

Among these inner solar system asteroids are Mars-crossing asteroids, which are defined as asteroids with perihelion distance greater than 1.3 AU and less than 1.666 AU. Asteroid 699 Hela (A910 LC), whose orbit we aim to refine in this work, is a Mars-crossing asteroid.

The orbits of asteroids can be described by six orbital elements: semi-major axis (a), eccentricity (e), inclination (i), longitude of ascending node (Ω), argument of perihelion (ω), and the mean anomaly (M). The values of the semi-major axis and eccentricity define the shape of the asteroid's orbit. More specifically, an orbit's semi-major axis is the distance from the center of the elliptical orbit to either of its two farthest points, while the eccentricity defines the degree of elongation of the ellipse. Additionally, the inclination, longitude of the ascending node, and the argument of perihelion describe the orientation of the orbit in space. The inclination is the angle between the plane of the asteroid's orbit and the ecliptic plane. Longitude of the ascending node is the angle measured eastward between the vernal equinox and the line of nodes: the line drawn between the two points at which the asteroid passes through the ecliptic plane (ascending and descending nodes). Argument of perihelion is the angle between the ascending node and the asteroid's point of perihelion. Mean anomaly defines an asteroid's current position as an angle past perihelion assuming a circular orbit.

We employed the method of Gauss to determine the orbital elements of 699 Hela. Gauss's method requires the right ascension and declination of the asteroid at three approximately equally-spaced observation times. From these three observations the six orbital elements can be determined. The remainder of this paper is devoted to the description of our observation-based determination of the orbital elements of asteroid 699 Hela.

II. METHODS

Here we briefly report on our observational processes, image reduction and data processing steps, and obser-

* Equal contribution.

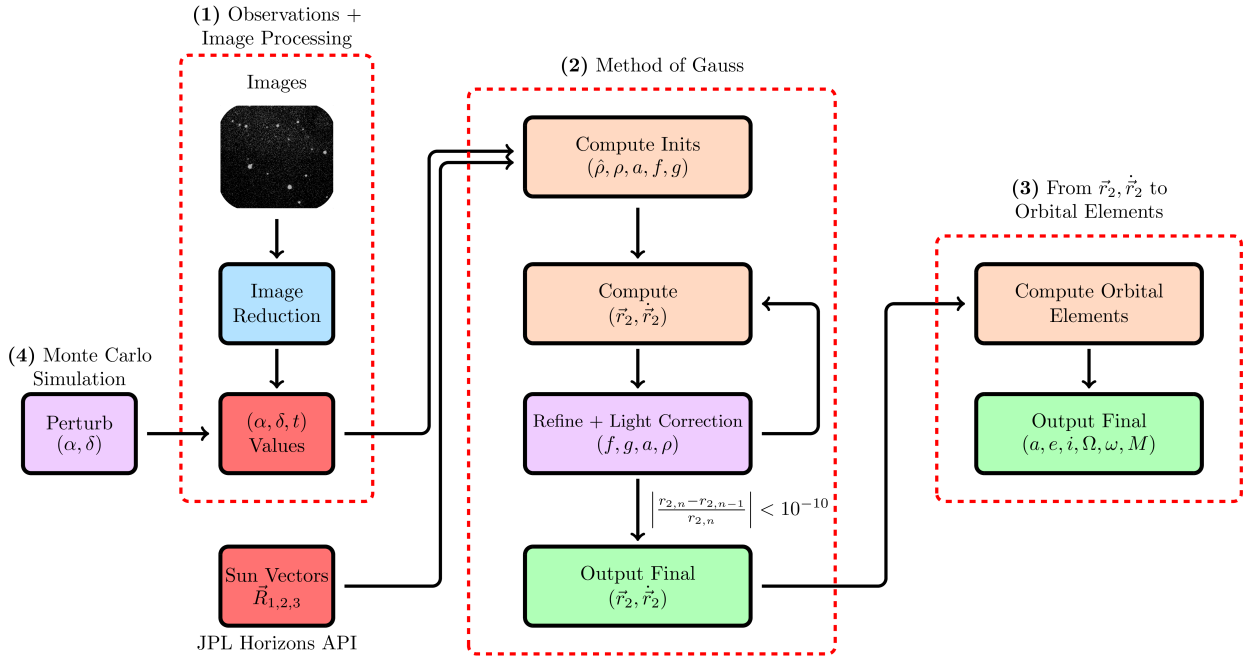

FIG. 1. Orbital element determination pipeline. Illustrates process of observations and the method of Gauss used to determine orbital elements.

vation error determination process. We then describe Gauss's method for orbit determination and introduce our implementation of this method in code to determine the orbit of asteroid 699 Hela. Lastly, we describe the process to compute the orbital elements from the outputs of Gauss's method and the Monte Carlo simulation necessary to determine uncertainties.

A. Observations and Image Processing

1. *Data Acquisition*

Observations of the 699 Hela asteroid were taken every other clear night at the Sommers-Bausch Observatory at the University of Colorado, Boulder, which is located at latitude 40°00′13.36″ N and longitude 105°15′46.84″ W. The principal instrument used in the observations was a 20-inch PlaneWave telescope, equipped with a ZWO ASI6200MM Pro camera. The 20-inch PlaneWave telescope is a reflecting telescope which utilizes two mirrors to collect light from objects in space and channel it into the camera lens. The primary mirror in the back of the telescope has a 20-inch diameter, while the secondary mirror has a diameter of 7.5 inches. We exclusively used the UV/IR(L) (Ultraviolet and Infrared) filter for data acquisition. This filter is used to block ultraviolet and infrared rays, which improves the sharpness of the images. The UV/IR(L) filter proves ideal for asteroid imaging as the asteroid can be dimmer than surrounding stars, making clarity in the image a necessary characteristic in identifying the object [7].

Time (yyyy/mm/dd hh:mm) [UTC]	Images Taken
2024 06 24 03:30 - 05:00	10 Flats; 6 Lights
2024 07 03 03:30 - 05:00	10 Flats; 9 Lights
2024 07 06 03:30 - 05:00	10 Flats; 9 Lights
2024 07 09 03:30 - 05:00	10 Flats; 12 Lights
2024 07 11 03:30 - 05:00	10 Flats; 9 Lights

TABLE I. Observation Journal. All observations taken from the Sommers-Bausch Observatory at the University of Colorado, Boulder.

It is ideal for Gauss' method to record the asteroid's position with equal time between observations. However, due to natural circumstances, this is not always possible. Table I includes the dates and times of all observations of this asteroid.

2. *Image Reduction*

To obtain the clearest images of the 699 Hela asteroid, careful reduction of the telescope images was required. Issues with raw images include dark current, vignetting from the telescope, hot pixels, cosmic rays, and dust. Dark current, cosmic rays, and hot pixels specifically can lead to inaccurate counts of photons within the CMOS sensors, causing incorrect values of magnitude for the asteroid. Following standard data reduction techniques, flat field images and darks were required to remedy these inaccuracies.

The reduced images were then used to compute the magnitude, right ascension, and declination of the aster-

oid. AstroImageJ (AIJ) and Astrometry software plate solving and image reduction tools were used for this step. By taking the images and comparing the star field to known star positions, the right ascension and declination of the stars and asteroid could be determined. By selecting stars in the image through SAOImage ds9, an imaging and data visualization software, and comparing the photon counts to their known magnitudes from the USNO UCAC4 catalog of stars, a graph of the linear regression between the photon count and known magnitudes could be made. With the regression data, an estimate for the asteroid's apparent magnitude could be made.

Algorithm 1 Method of Gauss with Light Correction

Input: $(\alpha_i, \delta_i, t_i)$, $i \in \{1, 2, 3\}$
Output: $\vec{r_2}$ and $\dot{\vec{r_2}}$
$\hat{\rho_i} \leftarrow \begin{bmatrix} \cos\alpha_i \cos\delta_i \\ \sin\alpha_i \cos\delta_i \\ \sin\delta_i \end{bmatrix}$
Require: $|\hat{\rho_i}| = 1$
$T_i \leftarrow t_i$
$\tau_{1,0,3} \leftarrow$ values computed with Equation (2).
$a_1, a_3 \leftarrow \frac{\tau_3}{\tau_0}, -\frac{\tau_1}{\tau_0}$
$\rho_{1,2,3} \leftarrow$ values computed with Equation (5).
$\vec{r_i} \leftarrow \rho_i\hat{\rho_i} - \vec{R_i}$
$\dot{\vec{r_2}} \leftarrow \frac{\tau_3\vec{v_{12}} - \tau_1\vec{v_{23}}}{\tau_0}$
$f_1, g_1, f_3, g_3 \leftarrow$ values computed with Equation (8) and Equation (9).
$a_1, a_3 \leftarrow \frac{g_3}{f_1 g_3 - f_3 g_1}, -\frac{g_1}{f_1 g_3 - f_3 g_1}$
$j \leftarrow 0$
while $\left|\frac{r_{2,n} - r_{2,n-1}}{r_{2,n}}\right| < 10^{-10}$ **and** $j < 500$ **do**
    $\rho_{1,2,3} \leftarrow$ values computed with Equation (5).
    $t_i \leftarrow T_i - \frac{\rho_i}{c}$ ▷ Light Correction
    $\vec{r_i} \leftarrow \rho_i\hat{\rho_i} - \vec{R_i}$
    $\vec{r_2} \leftarrow \frac{g_3\vec{r_1} - g_1\vec{r_3}}{f_1 g_3 - f_3 g_1}$
    $\dot{\vec{r_2}} \leftarrow \frac{f_3\vec{r_1} - f_1\vec{r_3}}{f_3 g_1 - f_1 g_3}$
    $f_1, g_1, f_3, g_3 \leftarrow$ refined values computed with Equation (8) and Equation (9).
    $a_1, a_3 \leftarrow \frac{g_3}{f_1 g_3 - f_3 g_1}, -\frac{g_1}{f_1 g_3 - f_3 g_1}$
    $j \leftarrow j + 1$
end while
return $\vec{r}, \dot{\vec{r}}$

3. Determination of Errors in Astrometry

Although the techniques to obtain the measured right ascension and declination of the asteroid provide close estimations of its location, there are still inaccuracies that need to be accounted for. The method used in this research was the Least Squares Plate Reduction (LSPR) technique. In this process the measured right ascension and declination of the asteroid is compared to the calculated value from JPL Horizons [8], and the plate solve from Astrometry software. Using the line of best fit between the two estimations for the position of the asteroid LSPR reports the uncertainties for both values. Table II shows the uncertainties in the values of 699 Hela's position in multiple values of the right ascension and declination. These uncertainties were then propagated to the final orbital elements with the Monte Carlo simulation to determine their specific uncertainties.

B. Orbit Determination

To determine the orbital elements of asteroid 699 Hela from the observational data with Gauss' method we followed the general pipeline outlined in Fig. 1. Essentially, we use Gauss' method to determine $\vec{r}_2, \dot{\vec{r}}_2$ (the position and velocity vectors of the asteroid at the middle observation) from the three observationally determined (α, δ, t) values of the asteroid, and then use these position and velocity vectors to determine the six orbital elements $(a, e, i, \Omega, \omega, M)$ at the middle observation—with these values, we may generate the ephemeris data for the asteroid at some future time.

With five observations of data, we chose one image from each observation to determine the asteroid's right ascension and declination (α, δ) from. As Gauss' method takes only data from three observations (i.e. supports only three values of (α, δ, t) input), we ran the ten combinations of input data to determine the "best" (closest to JPL Horizons) set of three observations for our orbital determination task. We ran Gauss' method on this set of three (α, δ, t) values for asteroid 699 Hela.

1. Method of Gauss

The method of Gauss [9] is useful for determining the position and velocity vectors of an asteroid at the middle observation given 3 sets of right ascension, declination, and time values (α, δ, t) corresponding to 3 observations.

To begin the method of Gauss, we first calculate the topocentric unit vectors $\hat{\rho}_i$ for each observation with

$$\hat{\rho}_i = \begin{bmatrix} \cos\alpha_i \cos\delta_i \\ \sin\alpha_i \cos\delta_i \\ \sin\delta_i \end{bmatrix}, \tag{1}$$

where α_i and δ_i are the right ascension and declination, respectively, at the i^{th} observation. We then calculate the gaussian time intervals τ_j as

$$\begin{aligned} \tau_1 &= k(t_1 - t_2) \\ \tau_0 &= k(t_3 - t_1) \\ \tau_3 &= k(t_3 - t_2), \end{aligned} \tag{2}$$

where t_i is the time in Julian days at the i^{th} observation and the constant $k = 0.0172020989484$ which is equal to the square root of the universal gravitational constant, G, and the mass of the sun, M. With these values for τ,

we may calculate initial values for a_1 and a_3 with

$$a_1 = \frac{\tau_3}{\tau_0} \tag{3}$$

$$a_3 = -\frac{\tau_1}{\tau_0}. \tag{4}$$

These values of a are useful for the computation of ρ, which are calculated as

$$\rho_1 = \frac{a_1(\vec{R_1} \times \hat{\rho_2}) \cdot \hat{\rho_3} - (\vec{R_2} \times \hat{\rho_2}) \cdot \hat{\rho_3} + a_3(\vec{R_3} \times \hat{\rho_2}) \cdot \hat{\rho_3}}{a_1(\hat{\rho_1} \times \hat{\rho_2}) \cdot \hat{\rho_3}}$$

$$\rho_2 = \frac{a_1(\hat{\rho_1} \times \vec{R_1}) \cdot \hat{\rho_3} - (\hat{\rho_1} \times \vec{R_2}) \cdot \hat{\rho_3} + a_3(\hat{\rho_1} \times \vec{R_3}) \cdot \hat{\rho_3}}{-(\hat{\rho_1} \times \hat{\rho_2}) \cdot \hat{\rho_3}}$$

$$\rho_3 = \frac{a_1(\hat{\rho_2} \times \vec{R_1}) \cdot \hat{\rho_1} - (\hat{\rho_2} \times \vec{R_2}) \cdot \hat{\rho_1} + a_3(\hat{\rho_2} \times \vec{R_3}) \cdot \hat{\rho_1}}{a_3(\hat{\rho_2} \times \hat{\rho_3}) \cdot \hat{\rho_1}}, \tag{5}$$

where $\vec{R_i}$ is the sun-earth vector at the time of the i^{th} observation determined with the JPL Horizons API. With these values we can calculate initial values of the position vectors $\vec{r_i}$ of the asteroid relative to the sun with

$$\vec{r_i} = \rho_i \hat{\rho_i} - \vec{R_i}. \tag{6}$$

With these position vectors, we may calculate an initial value for the velocity vector at the middle observation $\dot{\vec{r_2}}$ with

$$\dot{\vec{r_2}} = \frac{\tau_3 \vec{v_{12}} - \tau_1 \vec{v_{23}}}{\tau_0}, \tag{7}$$

where $\vec{v_{12}} = -\frac{\vec{r_2} - \vec{r_1}}{\tau_1}$ and $\vec{v_{23}} = \frac{\vec{r_3} - \vec{r_2}}{\tau_3}$. The $f(\tau)$ and $g(\tau)$ values can be calculated with $\vec{r_2}$ and $\dot{\vec{r_2}}$ as

$$f(\tau) = 1 - \frac{\tau^2}{2r_2^3} + \frac{(\vec{r_2} \cdot \dot{\vec{r_2}})\tau^3}{2r_2^5} + \frac{\tau^4}{24r_2^3}A \tag{8}$$

$$A = \frac{3\dot{r_2}^2}{r_2^2} - \frac{3}{r_2^3} - 15\left(\frac{\vec{r_2} \cdot \dot{\vec{r_2}}}{r_2^2}\right)^2 + \frac{1}{r_2^3}$$

$$g(\tau) = \tau - \frac{\tau^3}{6r_2^3} + \frac{(\vec{r_2} \cdot \dot{\vec{r_2}})\tau^4}{4r_2^5}, \tag{9}$$

where we look to calculate for $f_1 = f(\tau_1), g_1 = g(\tau_1), f_3 = f(\tau_3), g_3 = g(\tau_3)$. With these values we can compute an initial refinement of a_1 and a_3 before entering the iterative process of Gauss' method with

$$a_1 = \frac{g_3}{f_1 g_3 - f_3 g_1} \tag{10}$$

$$a_3 = -\frac{g_1}{f_1 g_3 - f_3 g_1}. \tag{11}$$

With these initial values for Gauss' method computed, we enter the iterative process of Gauss' method, which we describe in Algorithm 1. Note that to prevent the case where the sensitivity of 699 Hela's orbit prevents Gauss' method's loop from converging when the inputs are slightly perturbed in the Monte Carlo simulation, we add a counter to break the loop in that case and ignore those values. We also implemented light travel-time correction for our t_i values by computing

$$t_i = T_i - \frac{\rho_i}{c} \tag{12}$$

at every step in the loop, where T_i is the original measured t_i and ρ_i is the new computed earth-asteroid vector for each observation i.

Algorithm 2 Monte Carlo Simulation

Input: (α_i, δ_i), $i \in \{1, 2, 3\}$ and Number of Iterations N
Output: $(\sigma_a, \sigma_e, \sigma_i, \sigma_\Omega, \sigma_\omega, \sigma_M)$
Require: $N > 0$
Create 6 arrays, 1 for each orbital element.
for $i \in \{1, ..., N\}$ **do**
    $\alpha_n \sim \mathcal{N}(\alpha m, \sigma_\alpha)$
    $\delta_n \sim \mathcal{N}(\delta_m, \sigma_\delta)$
    $\vec{r}_n, \dot{\vec{r}}_n \leftarrow$ `GaussMethod`(α_n, δ_n)
    $a_n, e_n, i_n, \Omega_n, \omega_n, M_n \leftarrow$ `OrbitalElements`$(\vec{r}_n, \dot{\vec{r}}_n)$
    Append orbital element values to corresponding arrays.
end for
Take standard deviation of each array.
return $\sigma_a, \sigma_e, \sigma_i, \sigma_\Omega, \sigma_\omega, \sigma_M$

2. Orbital Element Determination

With the position $\vec{r_2}$ and velocity $\dot{\vec{r_2}}$ vectors at the middle observations determined via Gauss' method, we may compute the orbital elements $(a, e, i, \Omega, \omega, M)$ via properties of ellipses, the Vis-Viva equation, Kepler's laws, and basic trigonometry.

The semi-major axis a of the asteroid's orbit is calculated by rearranging the Vis-Viva equation:

$$a = \frac{1}{\frac{2}{r} - \frac{v^2}{\mu}}, \tag{13}$$

where $r = |\vec{r_2}|, v = |\dot{\vec{r_2}}|$ and $\mu = G(M_\odot + M_*)$ ($\mu = 1$ when distance is measured in AU and time in Gaussian days). The eccentricity e is calculated as

$$e = \sqrt{1 - \frac{h^2}{\mu a}}, \tag{14}$$

where $\vec{h} = \vec{r} \times \dot{\vec{r}}$ is the specific angular momentum vector. The inclination i is

$$i = \arccos\left(\frac{h_z}{h}\right), \tag{15}$$

where h_z is the z-component of the $\vec{h}$. The longitude of ascending node Ω is solved for with two equations such that a quadrant check is possible:

$$\sin\Omega = \frac{h_x}{h \sin i}$$
$$\cos\Omega = -\frac{h_y}{h \sin i}, \tag{16}$$

Date (yyyy/mm/dd.ddddd)	Julian Date	OD Use	Right Ascension (α)	Declination (δ)	Apparent Magnitude
2024 06 24.19541	2460485.69541		14h57m00.26s	-14°59'35.5"	14.59
2024 06 24.20252	2460485.70252		14h57m00.16s	-14°59'31.8"	14.43
2024 07 03.17262	2460494.67262		14h55m43.78s	-13°44'45.2"	14.72
2024 07 03.17574	2460494.67574		14h55m43.79s	-13°44'43.9"	14.55
2024 07 03.18385	2460494.68385		14h55m43.78s	-13°44'40.1"	14.58
2024 07 03.19129	2460494.69129		14h55m43.73s	-13°44'36.9"	14.51
2024 07 06.16485	2460497.66485		14h55m55.61s	-13°23'48.0"	14.54
2024 07 06.17181	2460497.67181	*	$14\text{h}55\text{m}55.64 \pm 0.55\text{s}$	$-13°23'45.2 \pm 0.35$"	14.56
2024 07 06.17817	2460497.67817		14h55m55.67s	-13°23'42.8"	14.56
2024 07 09.17368	2460500.67368		14h56m26.30s	-13°04'46.0"	14.96
2024 07 09.18297	2460500.68297		14h56m26.45s	-13°04'43.0"	14.66
2024 07 09.18896	2460500.68896	*	$14\text{h}56\text{m}26.47 \pm 0.44\text{s}$	$-13°04'41.3 \pm 0.33$"	14.63
2024 07 09.19642	2460500.69642		14h56m26.54s	-13°04'38.4"	14.62
2024 07 11.16323	2460502.66323	*	$14\text{h}56\text{m}56.77 \pm 0.37\text{s}$	$-12°53'19.4 \pm 0.29$"	14.77
2024 07 11.16019	2460502.66019		14h56m56.88s	-12°53'17.0"	14.82

TABLE II. Observation Data. All observations taken from the Sommers-Bausch Observatory in Boulder Colorado. Measurements of right ascension, declination, and apparent magnitude were gathered using a combination of the SAOImage ds9 and AIJ platforms. Uncertainties are included for the three observations used in our orbit determination (OD), which are marked with asterisks.

where h_x, h_y are the x, y-components of $\vec{h}$ respectively. To calculate the argument of perihelion ω, we compute the intermediate values U and ν, where U is the angle between $\vec{r}$ and the line of ascending nodes and ν is the true anomaly. The angle U is calculated

$$\begin{aligned} \sin U &= \frac{\hat{r}_z}{r \sin i} \\ \cos U &= \frac{x \cos \Omega + y \sin \Omega}{r}, \end{aligned} \tag{17}$$

where $\hat{r}_z$ is the z-component of the $\hat{r} = \frac{\vec{r}}{r}$ unit-vector and two equations are needed for a quadrant check to solve for U. The true anomaly ν is computed again with two equations for a quadrant check, where

$$\begin{aligned} \sin \nu &= \frac{a(1-e^2)}{he} \frac{\vec{r} \cdot \dot{\vec{r}}}{r} \\ \cos \nu &= \frac{1}{e} \left(\frac{a(1-e^2)}{r} - 1 \right). \end{aligned} \tag{18}$$

with U and ν, ω is simply calculated as:

$$\omega = U - \nu. \tag{19}$$

Lastly, the mean anomaly M, which is the only time-dependent orbital element, is computed by first computing the eccentric anomaly E:

$$\begin{aligned} \sin E &= \frac{r \sin \nu}{a\sqrt{1-e^2}} \\ \cos E &= \frac{ae + r \cos \nu}{a}, \end{aligned} \tag{20}$$

where we again need two equations for a quadrant check. After computing E, we compute M from Kepler's equation:

$$M = E - e \sin E. \tag{21}$$

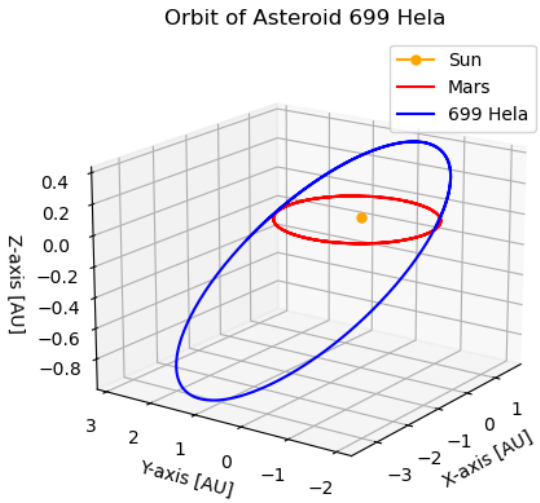

FIG. 2. Orbit visualization with `matplotlib.pyplot`. Three dimensional plot of the asteroid 699 Hela in comparison the Mars orbit, where the ecliptic plane is located at $Z = 0$.

3. *Monte Carlo Simulation*

To determine the uncertainties with the Method of Gauss and orbital element calculation, we ran a Monte Carlo simulation for 10^6 iterations. To run the Monte Carlo simulation, we take the 3 sets of (α, δ) values that we use for our orbital element calculation and perturb these values by sampling new values for right ascension and declination with $\alpha_n \sim \mathcal{N}(\alpha m, \sigma_\alpha)$ and $\delta_n \sim \mathcal{N}(\delta_m, \sigma_\delta)$, where (α_m, δ_m) are the measured right ascension and declination and (α_n, δ_n) are the "new" right ascension and declination values used at each new iteration of the Monte Carlo simulation and σ_α and σ_δ are the uncertainties in the right ascension and declination

Orbital Element	Symbol	Calculated Value	JPL Horizons Value
Semi-Major Axis	a	2.61 ± 0.12AU	2.61227AU
Eccentricity	e	0.410 ± 0.027	0.410
Inclination	i	$15.29 \pm 0.19^\circ$	15.30°
Longitude of Ascending Node	Ω	$242.50 \pm 0.12^\circ$	242.55°
Argument of Perihelion	ω	$91.4 \pm 2.2^\circ$	91.5°
Mean Anomaly	M	$321.1 \pm 4.1^\circ$	321.0°

TABLE III. Orbital Elements. Calculated values for orbital elements at Julian Date 2460500.68896 with uncertainties computed via Monte Carlo in comparison to orbital elements from JPL Horizons.

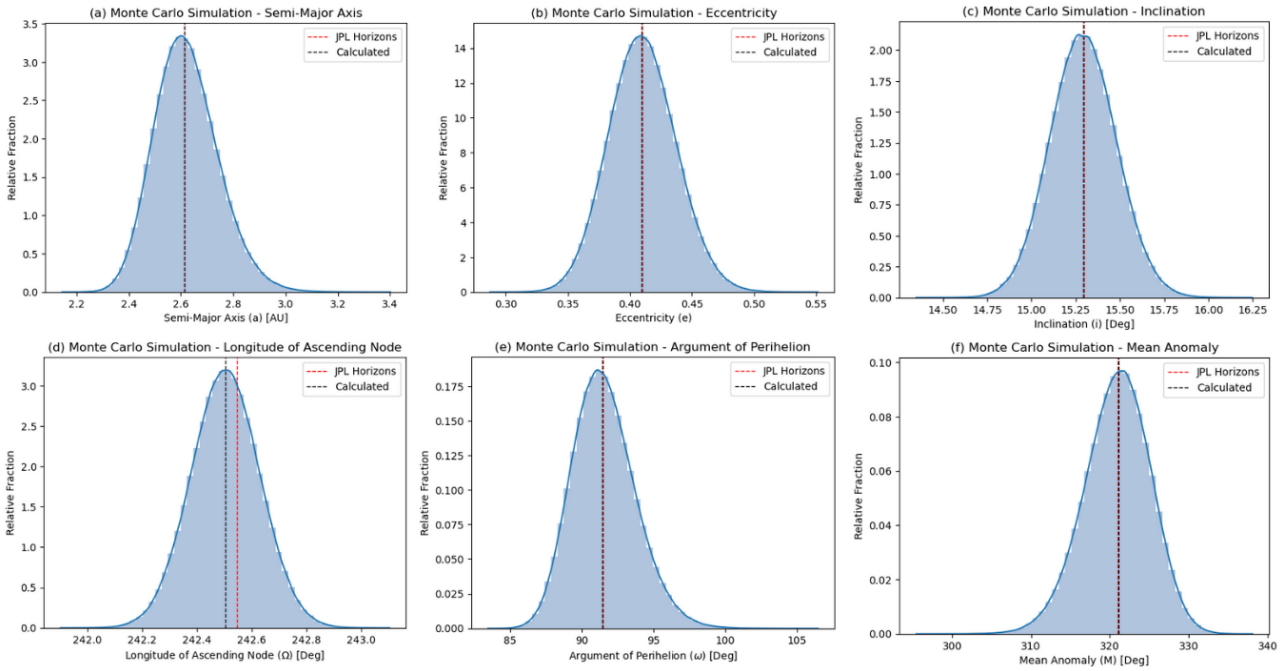

FIG. 3. Overview of Monte Carlo simulation results. **(a)** Semi-major axis results, **(b)** Eccentricity results, **(c)** Inclination results, **(d)** Longitude of the asscending node results, **(e)** Argument of perihelion results, and **(f)** Mean anomaly results. Calculated and JPL Horizons values for each orbital element are also identified.

measurement, respectively, that was determined from the Astrometry software `corr.fits` files.

At each iteration, we take these new values of right ascension and declination (α_n, δ_n) and run them through the Method of Gauss and orbital element computation steps and store the resulting list of orbital elements. We use the array of all of the different orbital elements generated by this process to determine the uncertainty by calculating the standard deviation σ for each of the different orbital elements. We describe this process in more detail in Algorithm 2.

To determine the accuracy of the Python code used to compute the orbital elements, a self-consistency check was required. From these orbital elements computed via the observations, a new ephemeris was generated for the right ascension and declination of the asteroid at the third observation, and these generated values were compared to the measured ones. Comparison between these measurements described the consistency of both the data and the code.

III. RESULTS

A. Observations and Image Processing

From the reduced images we used SAOImage ds9 and AIJ software to find the right ascension, declination, and apparent magnitude for asteroid 699 Hela. Table II outlines the date and time of each observation, along with the results from both applications of right ascension, declination, and apparent magnitude.

B. Orbit Determination

With the method of Gauss, the six orbital elements of the 699 Hela asteroid were determined. From these values, the orbit of 699 Hela is visualized in Figure 2. However, since the original input of the calculated right ascension and declination are prone to uncertainty, a Monte

Carlo simulation that can propagate the original uncertainty to the six orbital elements is necessary to determine the error in the final elements. Table. III shows the calculated orbital elements in addition to uncertainties obtained via Monte Carlo simulation.

The Monte Carlo simulation itself inputs slightly perturbed right ascension and the declination values into the orbit determination code which outputs the new, different, orbital elements. Assuming these new values would follow a Gaussian distribution centered at the measured (α, δ) values, this process was repeated 10^6 times, which produced the standard deviation of the elements that was interpreted as the uncertainty. Figure. 3 shows the resulting histograms from these simulations.

Moreover, the absolute magnitude of an asteroid can be determined according to

$$H = H(\alpha) + 2.5\log((1-G)\Phi_1(\alpha) + G\Phi_2(\alpha)) \quad (22)$$

$$\Phi_i(\alpha) = e^{\left(-A_i \tan(0.5\alpha)^{B_i}\right)}, \quad (23)$$

where H is the absolute magnitude, $H(\alpha)$ is the reduced magnitude, $i \in \{1, 2\}$, $A_1 = 3.33$, $A_2 = 1.87$, $B_1 = 0.63$, $B_2 = 1.22$, $G = 0.15$, and α is the phase angle. The reduced magnitude $H(\alpha)$ can be calculated based on the asteroid's visual magnitude V, the Earth-Sun distance r, and the Sun-asteroid distance ρ:

$$H(\alpha) = V - 5\log(r\rho), \quad (24)$$

where V is the visual magnitude calculated based on known visual magnitudes of surrounding stars in an image. Phase angle is determined according to the Law of Cosines:

$$\cos(\alpha) = \frac{r^2 + \rho^2 - R^2}{2r\rho}, \quad (25)$$

where R is the Earth-Sun distance. Using values from our middle observation, we determined that the absolute magnitude of asteroid 699 Hela is 11.2.

IV. DISCUSSION

The six orbital elements semi-major axis a, eccentricity e, inclination i, longitude of ascending node Ω, argument of perihelion ω, and mean anomaly M were determined based on right ascension and declination from three observations. The method of Gauss was used to determine the position $\vec{r_2}$ and velocity $\dot{\vec{r_2}}$ vectors of the asteroid at the middle observation, which were then used as the parameters to determine the orbital elements.

The self-consistency checks demonstrate code and data validity: we obtain low $\sim 1.079\%$ error in right ascension and $\sim 0.001\%$ error in declination on ephemeris generation consistency checks.

Comparison between our determined orbital elements and the orbital elements determined by JPL also reveal another layer of consistency. The percent differences between JPL values and our values for the orbital elements semi-major axis a, eccentricity e, inclination i, longitude of ascending node Ω, argument of perihelion ω, and mean anomaly M are low: 0.062%, 0.084%, 0.032%, 0.017%, 0.037%, and 0.0035%, respectively.

Error in the determination of the orbital elements may be due to error in astrometry and the unequal spacing of observations. To yield improvements in results, future work could consider corrections for stellar aberration and with the generation of higher order terms in the Taylor Series expansion used to determine position and velocity vectors (Equations (8) and (9)). Moreover, other techniques, such as differential corrections could be applied to yield further improvements in accuracy.

The results of this work are aimed to both refine the known orbital elements of asteroid 699 Hela as well as to contribute to the maintenance of a more accurate catalog of the orbits of planet-crossing asteroids as a whole.

CODE AVAILABILITY

An implementation of the described model for the orbit determination of asteroid 699 Hela and its results for orbital elements and Monte Carlo simulation are publicly available at `https://github.com/sdkyuanpanda/SSP-CUB-2024`.

ADDITIONAL INFORMATION

Competing interests The authors declare no competing interests.

Acknowledgements We wish to acknowledge the support of the SSP community and faculty with this report.

V. APPENDIXES

Appendix A: Reflection

- **Morgyn's Reflection**: Having no prior experience with a large research project like this, learning about astronomy and the way near earth asteroids are studied was completely unknown territory. However, I enjoyed the process of gathering measurements from our own asteroid and being able to reduce and process the images independently. The freedom and trust granted to us by SSP faculty enforced a learning environment which commanded growth through struggle and collaboration. Particularly, learning about the orbital elements and how the orbit of an asteroid is determined was enjoyable to contemplate. As a team, the three of us worked well together. Each of us brought our own set of skills to the table which created a well balanced

distribution of labour. SSP introduced me to various new techniques for solving complex problems. One of the newest skills the program required of me was the coding aspect. With no prior knowledge on coding, many of the assignments and OD code came with unique struggles, each teaching me how to navigate new situations. If I were to do anything differently in this program I would try to set aside some time to make sure I understood every concept. With such a complex system of variables, one misunderstanding can lead to numerous errors in the future.

- **Nicla's Reflection** - The orbit determination project was pleasantly challenging and new. The intricacy of each step of the project made it exciting to undertake. I appreciated the balance between classroom instruction and learning by doing. We collaborated online using Google Sheets and Overleaf. I particularly enjoyed data reduction and astrometry, putting together useful information for orbit determination and for the Minor Planet Center. I also enjoyed the programming involved in this project. It was an engaging first introduction to code for me. I liked seeing how we can use Python to make orbit determination much more efficient and reliable than orbit determination done by hand. Team Briezy had an even division of labor. During observations, we rotated roles; with data reduction sessions, we worked together to simultaneously reduce several nights of data; and while putting together the report, we each took on multiple responsibilities involving writing, coding, and revising. We worked well together, overcoming the challenges of limited time due to the rigorous schedule of SSP and of different levels of previous experience. If I were to do things again differently, I would do more planning ahead by inventing a better organization system for myself to arrange all the individual parts of the project.

- **Sam's Reflection** - I had fun. I like tikzpicture, coding, and LaTeX. We worked quite well together. I focused on writing the abstract, OD methods, making figures, and coding the Monte Carlo. I wish I didn't call the API repeatedly for the sun vector because that slowed down my code quite a bit lol. SSP was pretty cool :).

[1] Oortcloud, `https://science.nasa.gov/solar-system/oort-cloud/`, accessed: 2024-07-18.

[2] Comets, `https://science.nasa.gov/solar-system/comets/`, accessed: 2024-07-18.

[3] A. V. Sergeyev, B. Carry, M. Marsset, P. Pravec, D. Perna, F. E. DeMeo, V. Petropoulou, M. Lazzarin, F. La Forgia, I. di Petro, and Neorocks Team, Compositional properties of planet-crossing asteroids from astronomical surveys, **679**, A148 (2023), arXiv:2309.03555 [astro-ph.EP].

[4] A. Del Vigna, L. Dimare, and D. Bracali Cioci, The manifold of variations: impact location of short-term impactors, Celestial Mechanics and Dynamical Astronomy **133**, 10.1007/s10569-021-10024-w (2021).

[5] Asteroid Institute: Annual Progress Report 2023.

[6] P. Wiegert and B. Hyatt, Encounter circumstances of asteroid 99942 apophis with the catalogue of known asteroids (2024), arXiv:2403.00541 [astro-ph.EP].

[7] Optolong uv/ir cut, `https://www.optolong.com/cms/document/detail/id/146.html`, accessed: 2024-07-19.

[8] `https://ssd.jpl.nasa.gov/horizons/`, accessed: 2024-07-18.

[9] C. F. Gauss, *Theoria motus corporum coelestium in sectionibus conicis solem ambientium.* (Perthes und Besser, Hamburg., 1809).